Acta Cryst. (1978) A**34**, 542–547

The Electron Distribution of the Hydroxide Ion in Lithium Hydroxide

BY S. L. MAIR

CSIRO, Division of Chemical Physics, PO Box 160, *Clayton, Victoria, Australia* 3168

(*Received* 1 *November* 1977; *accepted* 27 *January* 1978)

Analysis of recently published X-ray and neutron diffraction data for LiOH reveals that there are pronounced non-spherical deformations of the electron density about the oxygen pseudo-atom. Comparison with a theoretical calculation of the electron density for the isolated hydroxide ion shows that these deformations are due to π-like bonding of the oxygen to the neighbouring hydrogen pseudo-atom. The observed features have shapes consistent with the non-spherical electron distribution of an isolated hydroxide ion undergoing rigid-body libration and translation. It is shown that an important effect of the rigid-body libration is a reversal in sign of the effective quadrupole component of the oxygen pseudo-atom electron density.

1. Introduction

LiOH crystallizes in the space-group $P4/nmm$ with cell dimensions $a = 3{\cdot}549$ Å, $c = 4{\cdot}334$ Å. The lithium atoms have point-group symmetry $\bar{4}2m$ and the oxygen and hydrogen atoms both have symmetry $4mm$ (see Fig. 1). Of the alkali hydroxides, LiOH is unique in that its abnormally long OH—OH separation (3·4 Å) precludes the formation of hydrogen bonds (Campbell & Coogan, 1965). This structural phenomenon makes LiOH particularly amenable to electron-density analysis, as it may be expected that for this system the bound hydroxide ion would resemble the isolated molecular ion, for which accurate *ab initio* wavefunctions exist. If the individual hydroxide ions indeed exist as partially independent units in the crystal, this would imply that rigid-body motion would form a large component of their total thermal movement. This conclusion is supported by the work of Coogan (1965), who obtained from lattice-energy calculations a librational frequency in agreement with infrared data.

Göttlicher & Kieselbach (1976) (hereafter G & K) have recently measured absolute X-ray diffraction intensities from LiOH single crystals at room temperature. The crystals were parallel-sided slabs, set to give symmetrical Laue diffraction. The thorough measurement procedure of G & K included experimental determination of the thermal diffuse scattering, secondary extinction and *Umweganregung* effects, their measurements extending out to $\sin\theta/\lambda = 1{\cdot}0$ Å^{-1}. By integrating over the resulting electron density, G & K estimated the electron population of the individual pseudo-atoms.* They further refined their data using pseudo-atom scattering factors parametrized in terms of anisotropic Gaussian functions.

G & K have also measured room-temperature neutron diffraction intensities for LiOH. These measurements supplement the earlier ones of Dachs (1959). Although the two sets of neutron-determined positional parameters (for oxygen and hydrogen) are in agreement, the thermal parameters show differences of almost 30%. Neither of the neutron diffraction experiments were carried out to the high level of accuracy of the X-ray experiment and, in fact, G & K did not use the neutron data in their electron-density analysis.

The present analysis of the electron density of LiOH takes an entirely different approach from that of G & K. In refining the X-ray data, the neutron positional parameters are employed, rather than the X-ray ones, and neutron thermal parameters are assumed for the lithium and hydrogen pseudo-atoms. The difference

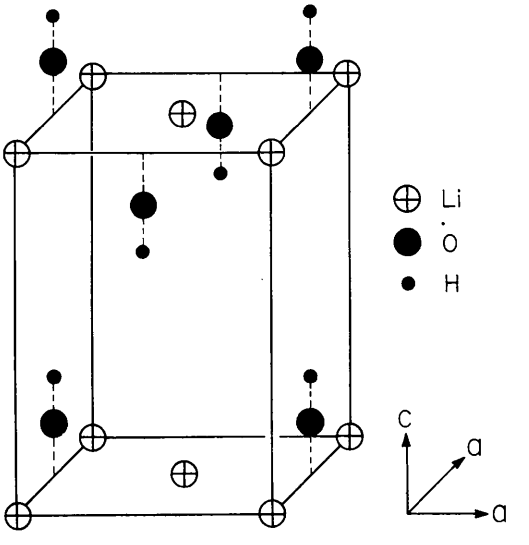

Fig. 1. The structure of LiOH. The c axis has length 4·334 Å.

* The concept of the pseudo-atom is used to represent the atom-like entities of which a solid is composed.

electron density is analysed as a series of multipoles, expanded about each nuclear site (Dawson, 1967; Stewart, 1976). Detailed comparisons are made with the theoretical difference electron density of the isolated hydroxide ion. In addition, the effect of rigid-body thermal motion on the electron distribution is assessed.

2. Analysis of neutron data

The neutron structure factors of G & K (Göttlicher, private communication) were re-analysed using more recent values of the coherent neutron scattering factors, b (Bacon, 1972). The 7% increased value of b for lithium has a significant effect on the Li^+ temperature factor, but all other parameters show minimal changes from those obtained by G & K. Further details and results of the neutron refinement are summarized in Table 1. The data were not considered to be sufficiently accurate to refine rigid-body as well as internal vibrational parameters. However, a plausible treatment of the rigid-body motion is given in § 4.

3. Analysis of X-ray data

Positional and thermal parameters

The values of the positional and thermal parameters obtained from the neutron data (Table 1) were initially used in the X-ray refinements. However, it became evident that the high-angle data were showing effects consistent with the oxygen temperature factor, β_{33}, being too large. An alternative explanation, that of a non-spherical electron distribution effect, was rejected as it would have implied large deformations of the electron-density near the nucleus. The oxygen thermal parameters were therefore obtained from a high-angle refinement ($\sin\theta/\lambda > 0{\cdot}8$ Å^{-1}) of the X-ray structure factors for which $(h + k)$ is odd. These structure factors depend almost entirely on the oxygen pseudo-atom core electrons. The values obtained for β_{11} and β_{33} (in the notation of G & K) for oxygen were, respectively, 0·36 and 0·57. The 16% decrease in β_{33} brings that parameter closer to the value obtained by Dachs (1959), suggesting that the high-angle neutron data of G & K contain a systematic error. The oxygen temperature factors have therefore been assigned the values determined from the high-angle X-ray refinement in all the results presented here.

Table 1. *Neutron data refinement*

Figures in parentheses show one standard deviation and refer to last significant figure. Unit weights were employed.

	Li	O	H
β_{11}*	0·38 (2)	0·34 (3)	1·28 (4)
β_{33}*	0·93 (5)	0·68 (2)	0·85 (4)
z*	–	0·1938 (4)	0·410 (1)
b†	−0·194	0·575	−0·372

Scale factor = 0·690 (6)

$$R = \frac{100\,\Sigma_i |F_o^i - F_c^i|^2}{\Sigma_i |F_o^i|^2} = 4{\cdot}2 \qquad R_w = \left[\frac{100\,\Sigma_i w_i (F_o^i - F_c^i)^2}{\Sigma w_i |F_o^i|^2}\right]^{1/2} = 4{\cdot}7$$

* Notation as for G & K.

† b = coherent scattering amplitude (10^{-12} cm).

Extinction

G & K corrected their data for secondary extinction, but made no primary extinction correction. A semi-empirical correction was therefore applied, based on equation (74) of Weiss (1966), for symmetrical Laue diffraction from an almost imperfect crystal. When secondary extinction is not present, this equation reduces to

$$|F_o|^2 = |F_c|^2 (1 - x\,|F_c|^2 K^2), \qquad (1)$$

where F_o and F_c are the observed and calculated absolute structure factors, K^2 is the polarization factor and x is a constant for an experiment at a given wavelength. The constant x was refined for LiOH to be $(7 \pm 1) \times 10^{-4}$ e^{-2}.

Weighting scheme

In the absence of detailed information about the errors associated with each structure factor, a unit weighting scheme was employed. A weighting scheme based upon the average errors indicated by G & K (*viz.* less than 1% for the strong reflections, 2–5% for the weak reflections) was rejected on the basis that the low- to medium-angle reflections, which contain the electron-density information, received relatively low weights. However, use of either weighting scheme led to similar results for the electron distribution.

Multipole expansion of pseudo-atom electron density for the OH^- *ion*

Stewart (1976) has outlined a method for representing the electron distribution in a crystal by a finite multipole expansion about each nuclear site. Such a multipole expansion has been used here to analyse the electron density of the OH^- ion in LiOH. Generalized radial scattering factors, obtained by a least squares fit to the Hartree–Fock–Roothaan one-electron molecular density function of the isolated OH^- ion, were used as radial functions. Stewart, Bentley & Goodman (1975) have outlined their method for obtaining such scattering factors for diatomic molecules, and R. F. Stewart (private communication) has derived [2/1] and [2/2] scattering factors calculated from the ($^1\Sigma^+$) OH^- wavefunction of Cade (1967). The notation $[n/m]$ refers to the order of the multipole expansion

about the oxygen (n) or hydrogen (m) pseudo-atom, 1 denoting a dipole and 2 a quadrupole as the last term in the expansion. Note that, to the quadrupole level of the multipole expansion, the OH^- fragment in the crystal has cylindrical symmetry. κ expansion parameters (see, for example, Coppens *et al.*, 1977) were refined for each scattering factor [defined by $f_n^l(\kappa_n^l s)$, instead of $f_n^l(s)$, where $s = \sin\theta/\lambda$ and i refers to the atomic species], including dipole and quadrupole functions. A κ refinement was also carried out for the Li^+ monopole. Amplitudes, D^l and Q^l, which scale the dipole and quadrupole scattering factors, respectively, were refinable parameters.

4. Interpretation of results

Fig. 2 shows the deformation electron density in the (100) plane obtained by subtracting theoretically calculated spherical distributions from the observed electron density. The spherical distributions correspond in this case to the isolated ions, Li^+ and O^-, and to the spherical bonded hydrogen atom of Stewart, Davidson & Simpson (1965). Scattering factors were obtained from *International Tables for X-ray Crystallography* (1974).

The deformation density has pronounced features at the Li^+ sites and in the vicinity of the OH^- ion, but is quite flat throughout the rest of the unit cell, indicating that there is little noise in the data. The lithium difference distribution is almost spherical, and may reflect a genuine contraction of the isolated-ion electron distribution, or alternatively may be caused by the temperature factors being too high. In the vicinity of the hydrogen there is evidence of the expected dipole component in the electron density, indicating a concentration of electron density in the bonding direction. It is the aspherical negative region about the O^- ion, and the adjacent diffuse positive area, which undoubtedly form the most interesting features in the total distribution.

A naive approach to the bonding between the O^- and H pseudo-atoms would perhaps lead to the expectation that there would be an accumulation of electron density between the oxygen and hydrogen atoms, corresponding to σ-type bonding. However, the effect of a hydrogen on an isolated O^- ion is to polarize the electron distribution of the latter in such a way that the dominant non-spherical feature is characteristic not of σ bonding, but rather of a π-bonding distribution. This is clear from the deformation electron density of the isolated molecule, OH^- ($^1\Sigma^+$), shown in Fig. 3. This deformation density was calculated using the wavefunction of Cade (1967) to obtain the electron density of OH^-, from which the same spherical O^- and H distributions as for Fig. 2 were subtracted. The isolated molecule shows axial depletion of the electron density about the oxygen, as in Fig. 2, and a diffuse positive torus of electron density perpendicular to the axis, redistributions which characterize π bonding.

A quantitative comparison between Figs. 2 and 3 is provided by Table 2, which contains the results of the multipole expansion refinements of the electron distribution in LiOH. In these refinements the O^- and H scattering factors were based on the isolated OH^- molecule, as described in the previous section. The marginal significance of the hydrogen quadrupole term did not warrant use of the [2/2] basis, so that results

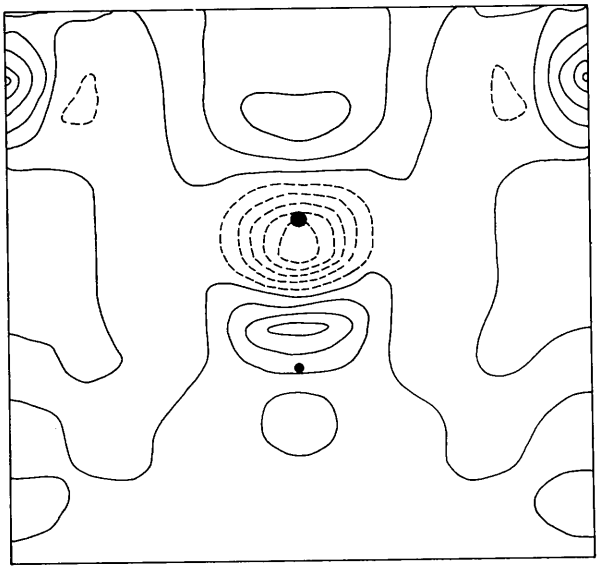

Fig. 2. The observed difference density of LiOH in the (100) plane. Spherical atoms, as described in the text, have been subtracted out. Contour interval is 0·13 e $Å^{-3}$, with negative contours broken. The oxygen is represented by the larger black disc, the hydrogen by the smaller one, and the lithiums by the two open semicircles at the upper edges of the contour map.

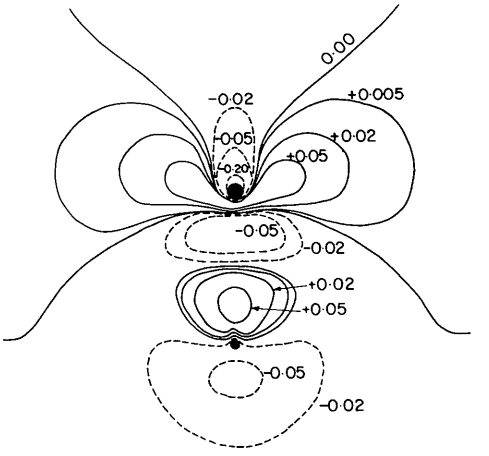

Fig. 3. The calculated difference density for the static isolated OH^- molecular ion. Spherical atoms have been subtracted out, as in Fig. 2. The contour intervals are maked in e $bohr^{-3}$ (1 e $bohr^{-3}$ = 6·8 e $Å^{-3}$). The oxygen and hydrogen are represented as in Fig. 2.

using the [2/1] basis set only are presented. The [2/1] radial functions for the isolated OH^- molecule are shown in Fig. 4.

From Table 2 it can be seen that addition of the non-spherical terms to the model improves the fit significantly, without, perhaps, providing the ultimate description of the electron distribution. Examination of the third and fourth rows of numbers enables one to compare the static isolated hydroxide molecule with the molecule bound in LiOH. The most striking difference between the two cases is in the opposite signs of the apparent oxygen quadrupole components. This is confirmed by examination of Figs. 2 and 3. In Fig. 2 the negative region about the O^- site is flattened perpendicular to the c axis, whereas in Fig. 3, it is more elongated in the axial direction. Corresponding opposite effects exist for the positive regions.

An explanation for the reversal in sign of the quadrupole term can be made in terms of the highly probable presence of rigid-body motion of the OH^- ion in LiOH (see *Introduction*). An estimate for the mean-square vibrational and librational parameters can be obtained from the refined thermal parameters under the following assumptions:

(1) The rigid-body translational motion is that refined for the oxygen pseudo-atom.

(2) There is no correlation between librational and translational motion, and libration is about the centre of mass, which is located close to the oxygen nucleus.

(3) The residual non-rigid-body vibration of the hydrogen pseudo-atom is isotropic. Such non-rigid-body motion is allowable when one considers that the hydrogen is actually moving in the field of all its neighbours, not just as part of an isolated OH^- unit.

Then one obtains for the mean-square rigid-body displacements in the x and z directions:

$$\overline{U_1^2} = 0{\cdot}018\ \text{Å}^2,\ \overline{U_3^2} = 0{\cdot}029\ \text{Å}^2$$

and for the mean-square angular displacement

$$\overline{\theta^2} = 0{\cdot}044\ (\text{radians})^2, \text{ corresponding to } (\overline{\theta^2})^{1/2} = 12°.$$

These values are comparable to those derived by Coogan (1965).

Appropriate Gaussian thermal smearing functions were defined using the above values, and these were convoluted with the static electron distribution of Fig. 3. The convolution was achieved by a numerical procedure using Gauss–Hermite integration (*Handbook of Mathematical Functions*, 1965). The resulting dynamic distribution is presented in Fig. 5. The deformation density map shows features which are qualitatively quite similar to the observed deformation density of Fig. 2. In particular, the quadrupole component of O^- is now of the same sign in both maps. This is due to the librational component of the rigid-body motion, which preferentially smears the diffuse features (*i.e.* those distant from the oxygen site). The librational motion need not be as large as that used in Fig. 5. If $\overline{\theta^2}$ is reduced by a factor of two the reversal in sign of the quadrupole contribution still occurs.

In making further comparisons between Figs. 2 and 5 several factors should be kept in mind:

(1) The significant non-rigid-body vibration of the hydrogen is not included in Fig. 5.

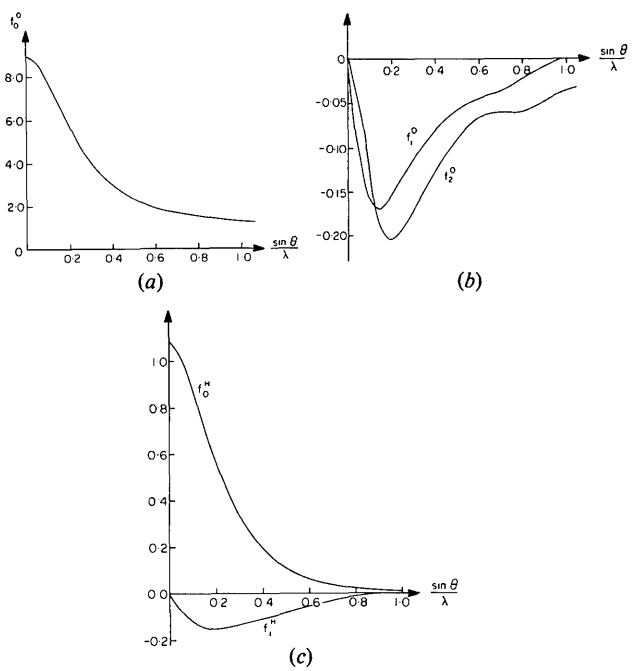

Fig. 4. The [2/1] radial functions supplied by Stewart for the isolated OH^- ion: (*a*) f_0^O, (*b*) f_1^O and f_2^O, (*c*) f_0^H and f_1^H.

Table 2. *Refinement of* LiOH *data using* [2/1] *fit to isolated* OH^- *for radial-scattering-factor basis functions of* O^- *and* H

R_w and R as defined in Table 1. Figures in parentheses as in Table 1. In the agreement parameter at right n = number of observations, m = number of parameters varied.

	Lithium	Oxygen					Hydrogen					
	κ_0	κ_0	D	κ_1	Q	κ_2	κ_0	D	κ_1	R_w	R	$\left(\frac{\sum_l w_l \lvert F_o^l - F_c^l \rvert^2}{n-m}\right)^{1/2}$
Refining only spherical components	0·92 (3)	1·020 (5)	0·0	–	0·0	–	0·82 (4)	0·0	–	5·5	4·5	0·122
Refining all multipoles	0·93 (3)	1·020 (6)	1·2 (3)	0·8 (2)	−2·9 (6)	2·6 (2)	0·85 (5)	1·4 (3)	0·29 (1)	4·4	3·7	0·103
Values for isolated OH^-	–	1·0	1·0	1·0	1·0	1·0	1·0	1·0	1·0	–	–	–

(2) Librational motion will cause the neutron-determined O—H separation to be too small by up to 6%. This error in hydrogen position may account for the rather small value of κ_1^H (see Table 2). Further distorting effects of librational motion are not included in the calculated structure factors used to obtain Fig. 2, making detailed comparisons with Fig. 5 difficult to interpret.

(3) The O—H separations are probably not the same in the isolated and bound OH^- ions, though they are quite similar (0·936 Å in LiOH, before increase due to libration; 0·942 Å in isolated molecule).

(4) Small effects due to series termination will be present in Fig. 2.

(5) The other ions, both positive and negative, in the solid will perturb the isolated OH^- electron density. This may account for the generally larger peak heights in the observed map compared with the calculated one.

5. Discussion

This analysis of LiOH has allowed the determination of the essential qualitative features of the electron distribution of the OH^- ion. A full quantitative analysis would, however, require more accurate neutron data in order to determine more exactly the rigid-body and non-rigid-body thermal parameters. Alternatively, low-temperature X-ray and neutron data would be of great value. Nevertheless, the available data has enabled us to show that the O—H bond has strong π-like character, the bound hydroxide molecule being qualitatively similar to the corresponding rigidly librating and vibrating isolated molecule. In the deformation density map, the characteristic feature of the π bonding is the negative area about the oxygen pseudo-atom extending into the region between the oxygen and hydrogen atoms. Similar effects, less distorted by libration, have been observed in cases where oxygen is terminally bonded to a large molecule, *e.g.* the three partial double N—O bonds in *p*-nitropyridine *N*-oxide (Coppens & Lehmann, 1976), suggesting that π bonding may be common in O—*X* configurations. The relative importance of π compared with σ bonding in the heavier first-row diatomics has been discussed by Hirshfeld & Rzotkiewicz (1974). They attribute this increased importance to the weakening effect on σ bonds of both the Pauli exclusion principle and the presence of radial nodes (which are absent for first-row π orbitals).

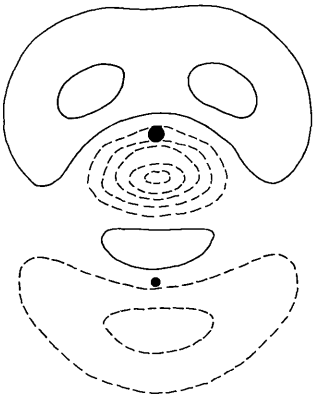

Fig. 5. The calculated difference density for the OH^- molecule with rigid-body motion consistent with the data for LiOH. Contour interval is 0·07 e Å^{-3}, with negative contours broken. The oxygen and hydrogen atoms are represented as in Fig. 2.

The distorting effect of thermal motion on the shape of the electron density is particularly severe for the hydroxide ion of LiOH. Thus libration about a centre nearly located on the oxygen nucleus causes a reversal in sign of the apparent quadrupole component of the oxygen electron density. In such cases the use of generalized scattering factors derived from static isolated diatomic molecules may be misleading if the effect of thermal motion is not clearly defined.

In a rigorous treatment of the structure factor for an assembly of librating molecules, it is not sufficient to regard the motion of the whole pseudo-atom as that of its nucleus (Schomaker & Trueblood, 1968), but one should rather integrate over each point in the distribution. This is particularly important for pseudo-atoms located close to the centre of libration. In such cases the orientation of the pseudo-atom multipoles will change with libration, and correction terms analogous to those derived for the dynamic molecular scattering factors by Stevens, Rys & Coppens (1977) [see their equation (20)] will have increasing effect.

Especial thanks are due to Professor S. Göttlicher for making available his structure factor data and details of his experiments, and to Professor R. F. Stewart for specially computing generalized scattering factors appropriate to this problem. I am indebted to Drs A. McL. Mathieson, S. W. Wilkins and C. K. Coogan for useful discussions, to Mr C. H. J. Johnson for assistance with numerical procedures and to Mr J. McAdam for some of the computer programs.

References

Bacon, G. E. (1972). *Acta Cryst.* A**28**, 357–358.
Cade, P. E. (1967). *J. Chem. Phys.* **47**, 2390–2406.
Campbell, I. D. & Coogan, C. K. (1965). *J. Chem. Phys.* **42**, 2738–2746.
Coogan, C. K. (1965). *J. Chem. Phys.* **43**, 823–830.
Coppens, P. & Lehmann, M. S. (1976). *Acta Cryst.* B**32**, 1777–1783.
Coppens, P., Yang, Y. W., Blessing, R. H., Cooper, W. F. & Larsen, F. K. (1977). *J. Am. Chem. Soc.* **99**, 760–766.
Dachs, H. (1959). *Z. Kristallogr.* **112**, 60–67.
Dawson, B. (1967). *Proc. R. Soc London, Ser. A.* **298**, 255–263.
Göttlicher, S. & Kieselbach, B. (1976). *Acta Cryst.* A**32**, 185–192.

Handbook of Mathematical Functions (1965). Edited by M. ABRAMOWITZ & I. A. STEGUN, p. 924, New York: Dover.

HIRSHFELD, F. L. & RZOTKIEWICZ, S. (1974). *Mol. Phys.* **27**, 1319–1343.

International Tables for X-ray Crystallography (1974). Vol. IV. Birmingham: Kynoch Press.

SCHOMAKER, V. & TRUEBLOOD, K. N. (1968). *Acta Cryst.* B**24**, 63–76.

STEVENS, E. D., RYS, J. & COPPENS, P. (1977). *Acta Cryst.* A**33**, 333–338.

STEWART, R. F. (1976). *Acta Cryst.* A**32**, 565–574.

STEWART, R. F., BENTLEY, J. & GOODMAN, B. (1975). *J. Chem. Phys.* **63**, 3786–3793.

STEWART, R. F., DAVIDSON, E. R. & SIMPSON, W. T. (1965). *J. Chem. Phys.* **42**, 3175–3187.

WEISS, R. J. (1966). *Selected Topics in Solid State Physics*, Vol. VI, edited by E. P. WOHLFARTH. Amsterdam: North Holland.

Acta Cryst. (1978). A**34**, 547–550

Piezoelectric, Electro-optic, Dielectric, Elastic and Thermoelastic Properties of Hexagonal $Cs_2S_2O_6$, $LiClO_4.3H_2O$, $LiClO_4.3D_2O$, and $Ba(NO_2)_2.H_2O$

BY S. HAUSSÜHL

Institut für Kristallographie der Universität zu Köln, 5000 *Köln* 1, *Zülpicher Strasse* 49, *Federal Republic of Germany*

(*Received* 15 *December* 1977; *accepted* 24 *January* 1978)

Complete tensor sets of piezoelectric, electro-optic, dielectric, elastic and thermoelastic properties were measured on hexagonal $Cs_2S_2O_6$, $LiClO_4.3H_2O$, $LiClO_4.3D_2O$, and $Ba(NO_2)_2.H_2O$. The space-group symmetry of $Cs_2S_2O_6$ and $Ba(NO_2)_2.H_2O$ has been definitely established, by X-ray work in combination with the measurement of polar properties, to be $P6_3mc$ and $P6_1$ ($P6_5$), respectively, contrary to earlier X-ray determinations. $LiClO_4.3H_2O$ and $LiClO_4.3D_2O$ possess almost identical physical properties, with the exception of density and density-dependent properties. The very small differences correspond to those observed in other hydrates and deuterates. Most components of the piezoelectric and electro-optic tensors do not exceed the effective values of other crystals already in technical use. However, an exceptionally strong longitudinal piezoelectric effect is observed in $Cs_2S_2O_6$ ($d_{333} = -41$ e.s.u. dyn^{-1}, electromechanical coupling coefficient k_t − 0·25), which together with other favourable acoustic and optical properties supports the application of this new material for acousto-optical devices in the high-frequency range.

Hitherto only a few polar crystals with hexagonal symmetry have been investigated with respect to their macroscopic properties. In this paper complete tensor sets of electrical and mechanical properties of four polar hexagonal crystals are reported. They all are easily obtained from aqueous solutions as large single crystals of high optical quality, and therefore deserve further consideration for applications in technical devices. Preliminary piezoelectric tests had revealed that the point symmetry for $Cs_2S_2O_6$ given in the literature as 62 (Hägg, 1932) is incorrect. Therefore, the symmetry properties of all four species had to be checked by X-ray diffraction and macroscopic properties. Some properties of $Ba(NO_2)_2.H_2O$ have already been reported by Gladkii & Zheludev (1967), but not all in complete tensor sets.

Crystal growth and measurements

Single crystals with diameters up to several cm have been grown from aqueous solutions by the usual evaporation technique at constant temperature. The growth experiments were carried out between 30 and 40 °C with resulting growth rates of *ca* 0·3 mm d^{-1}. The starting materials were produced by standard chemical processes: $Cs_2S_2O_6$ by reaction of Cs_2SO_4 with an aqueous solution of $BaS_2O_6.2H_2O$; $LiClO_4.3D_2O$ by dissolution of dehydrated $LiClO_4$ in D_2O; $Ba(NO_2)_2.H_2O$ by crystallization from an aqueous solution of $NaNO_2$ and $BaCl_2$ at *ca* 5 °C and manual selection of the yellowish crystals. The observed forms, ordered by their morphological rank, are listed in Table 1.